Konrad-Zuse-Zentrum
für Informationstechnik Berlin

Takustraße 7
D-14195 Berlin-Dahlem
Germany

WOLFGANG KÜHN, MANFRED KORZEŃ, OLAF PAETSCH

Fast Data Assimilation in Fire Tests of Steel Members

Preprint SC 98-33 (December 1998)

Fast Data Assimilation in Fire Tests of Steel Members

Wolfgang Kühn Manfred Korzeń* Olaf Paetsch

January 13, 1999

Abstract

This report presents a fast data assimilation method to produce an interpolating time and space temperature distribution for steel members subject to fire testing. The method assimilates collected temperature data into the numerical integration of the heat equation. This physically based method also allows the computation of lateral and axial heat flux into and inside the member.

Keywords: data assimilation, heat equation
Primary MSC: 35K05
Secondary MSC: 65M06

1 Introduction

Fire tests are performed to determine the contribution made by applied protection systems to the fire resistance of structural steel members such as beams and columns. These tests are usually required by law and are specified in test codes for the respective country, for example in [3] for Germany.

The fire protection system is evaluated according to the length of the fire resistance period, during which a design temperature of 500C° [3] or 750C° [8] on the steel surface is not exceeded.

The steel temperature is measured along the member at measurement stations. Each measurement station consists of 2 [3] or 5 [8] thermocouples to guard for thermocouple failure or abnormal behavior of fire protection. The required number of measurement stations are 3 [3] and 5 [8]. The required length of a member exposed to heat is 4000mm for beams and 3000mm for columns. With a typical lateral dimension between 245mm and 300mm, the members a rather slim (ratio of lateral to axial dimension less than 1:10).

The thermocouple locations throughout the member are very sparse and non-uniform. It is therefore desirable to interpolate the collected thermocouple data to obtain a temperature distribution throughout the member. This could be done by treating the problem as a pure interpolation problem, and can therefore be solved by standard techniques such as splines or scattered data interpolation. However, our aim is not simply to find a smooth and visually pleasing interpolant. Instead, by relating the data to its physical origin, we will be able to

*Bundesanstalt für Materialforschung und -prüfung

- compute an interpolant which is closer to the actual temperature distribution, and
- deduce other physical qualities of interest, such as the lateral and axial heat flux.

To advance beyond a direct data interpolation problem, the member together with the fire protection system is embodied in a computer model. In particular, knowledge of time evolution is embodied in a forecast model. This enables us to use observations distributed in time. Assimilation is the process of finding the model representation which is most consistent with the observations.

Our model is based on a non-linear, transient heat equation. The boundary condition in form of the unknown heat flux into the member has to be determined in a data assimilation step from the collected thermocouple data. By using an explicit, full time and space discretization of the heat equation alternately on a fine and coarse grid, we are able to achieve a very fast data assimilation. This will facilitate real-time data processing even in slow computational environments.

Data assimilation is mainly used in computational meteorology and oceanography [4]. As an inverse problem [1] it is related to parameter identification. Although both share a common objective, the term parameter identification is used when a small number of slow varying unknowns, for example material properties, have to be determined. On the other hand, we refer to data assimilation if part of the state of a dynamical system itself is unknown. We should also mention its links to optimal control [2][6] and the Kalman Filter [5].

This report will use a 1-D non-linear heat equation as a mathematical model for the member. However, the ideas presented in this report also carry through in 2-D or 3-D. The reduction to a 1-D model is acceptable for two reasons. First, one can observe that the lateral temperature variation is small, usually less than 10C°. Second, the required number of measurement stations is far too small to resolve the lateral temperature distribution. In fact, a member with ratio 1:10 already needs 21 measurement stations to acquire equal lateral and axial resolution.

The method in this report is applicable indiscriminately to the section type. It can be applied to 'I', 'H', angle or 'T' sections. It may also be applied to structurally hollow sections such as in circular or square members.

The fire protection system is specified by the type of material, by its thickness, and by the method the material is applied to the member (profiled or boxed). At this stage of the project, the nature of the fire protection system was not taken into consideration. The reason for this omission is that the resulting heat flux into the member is automatically determined by the collected temperature data and does not have to be conjured from the, possibly complex, heat transport processes occurring in the protection material.

An important part of fire testing is the assessment of the fire protection thickness by interpolating collected data over a range of fire protection materials and a range of steel sections. To conduct such an assessment, an understanding of the heat transport process is essential. This shall be a future part of the project.

The methods in this paper should be applied with care to very thin, usually sprayed on, fire protection material, and to reactive fire protection material. In these cases, the temperature distribution on the member can vary considerably both in time and space during fire testing, and the interpolation may thus be of very poor quality.

2 Symbols and Material Properties

symbol	**property**	**typical values at** 100C°
c_v	specific heat capacity	487J/kgK
ρ	density	7850kg/m^3
k	conductivity	50J/m K sec

Table 1: Temperature Dependent Material Properties for Steel

symbol	**definition**
c	$c_v \rho$
t_n	sampling time, $n = 1, \ldots, N$
Δt_n	time step $t_{n+1} - t_n$
x_j	point on discretization grid, $j = 1, \ldots, J$
Δx_j	grid spacing $x_{j+1} - x_j$
Σ_d	FTCS discretization grid
Σ_m	measurement (thermocouple) grid
f_j^n	value of function $f(x,t)$ at time t_n and location x_j
$u(x,y,z,t)$	time dependent temperature field
L	length of member
Ω	section of member
$A(\Omega)$	section area
γ	normal lateral heat flux [J/sec m^2]
Γ	average lateral heat flow line density [J/sec m]
Γ_{total}	total heat flux [J/sec]
u_l	lower mount temperature
u_u	upper mount temperature
u_f	furnace temperature
λ	fire protection material heat transfer coefficient

Table 2: Symbols

Whenever possible, we will suppress functional argument, such as in $u = u(x,y,z) = u(x,y,z,t)$.

3 Mathematical Model

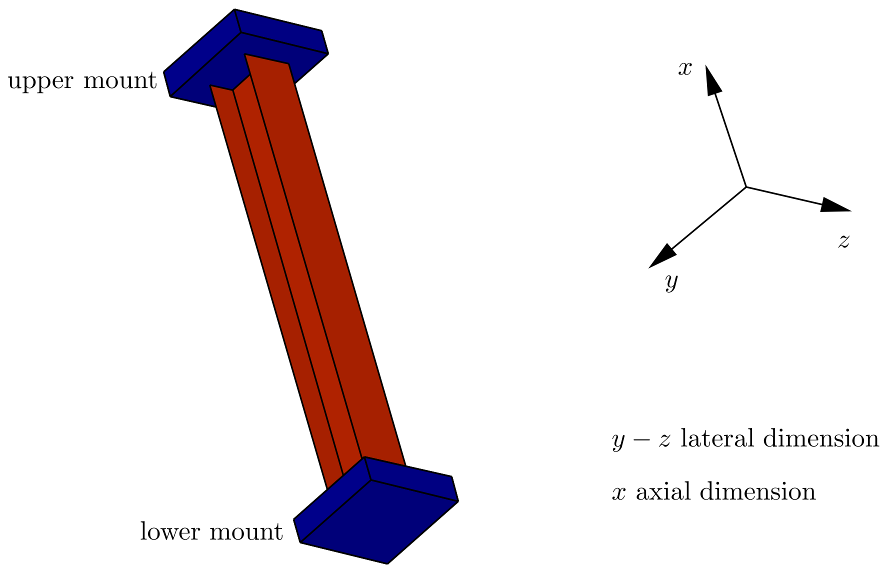

Figure 1: Beam with Slabs and Coordinate System

Let the surface of the member be partitioned into three disjoint sets $S_l \cup S_u \cup S_n$, where S_l and S_u are the contact surfaces with the lower and upper mount, respectively. Then a mathematical model for the member is the non-linear 3-D heat equation

$$c_v \rho \partial_t u = \nabla(k \nabla u),$$

with prescribed Dirichlet boundary conditions at the mounts

$$u\big|_{S_l} = u_l, \qquad u\big|_{S_u} = u_u,$$

Von Neuman boundary conditions throughout S_n, i.e. the normal heat flux into the member

$$k \partial_n u\big|_{S_n} = \gamma,$$

and an initial distribution $u\big|_{t=0} = u_0$ We assume that the mount temperatures u_l and u_u are collected and therefore known at all times. The mounts may be water cooled.

4 Reduction to 1-D Non-Linear Heat Equation

Let Ω be the $y-z$ section of the member and $A(\Omega)$ its area, see Figure 2. Define the mean section temperature by

$$v(x,t) = \frac{1}{A(\Omega)} \int_\Omega u(x,y,z,t)\, dA$$

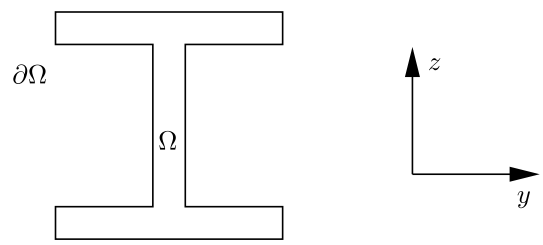

Figure 2: Section of Member

with $dA = dydz$. As shown in the Appendix, v then approximately satisfies the non-linear, 1-D heat equation

$$c\partial_t v = \partial_x(k\partial_x v) + \Gamma, \tag{1}$$

where $c = c_v\rho$ and Γ is the average lateral heat flux

$$\frac{1}{A(\Omega)}\int_{\partial\Omega}\gamma\, ds.$$

Note that $\Gamma = \Gamma(v, x, t)$ plays the role of an effective heat source in Eq. (1) and that $A(\Omega)\Gamma$ is the lateral heat flow line density.

5 Time and space discretization of heat equation

Equation (1) is discretized using a forward time, centered space (FTCS) scheme. The time grid is naturally given by the data acquisition system, which reads in thermocouple data at discrete times t_n, $n = 1, \ldots, N$. For space discretization, define a discretization grid

$$\Sigma_d = \{\, x_1, \ldots, x_J \,\}$$

consisting of J grid points such that the thermocouple locations Σ_m form a subset of Σ_d, see Fig. 3. Note that for a given thermocouple configuration Σ_m, the grid Σ_d is non-uniform in general.

On the discretization grid, the discrete temperature distribution $v_j^n = u(x_j, t_n)$ is defined. Note that v_1^n and v_J^n are the collected lower and upper mount temperatures, respectively. The FTCS representation of (1) is

$$c_j^n \frac{v_j^{n+1} - v_j^n}{\Delta t_n} = \frac{K_j^n \frac{v_{j+1}^n - v_j^n}{\Delta x_j} - K_{j-1}^n \frac{v_j^n - v_{j-1}^n}{\Delta x_{j-1}}}{\Delta x_j + \Delta x_{j-1}} + \Gamma_j^n, \tag{2}$$

where $K_j^n = k(v_{j+1}^n) + k(v_j^n)$ and $c_j^n = c(v_j^n)$. To solve (2) iteratively in time, the stability criterion

$$\max_{j,n} \frac{2\Delta t_n K_j^n}{c_j^n \Delta x_j^2} \le 1 \tag{3}$$

has to be satisfied, see [9]. The grid Σ_d should be chosen as fine as the resolution for the interpolant v_j^n is desired, but in accordance with the stability criterion

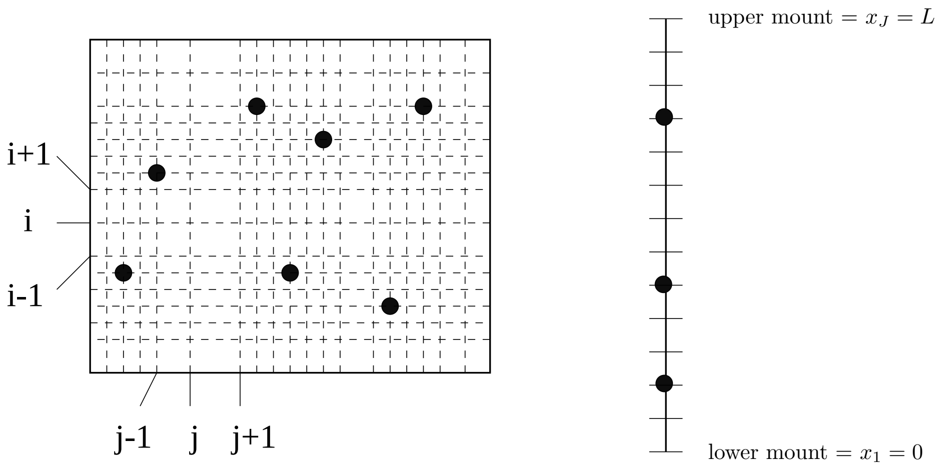

Figure 3: Scattered thermocouple locations Σ_m ($\bullet$) and non-uniform, finite difference (FD) grid Σ_d for 2D (left) and 1D (right)

(3). Substituting the values of Table 1 and a typical value of $\Delta t_n = 10\,\text{sec}$ into (3) gives $\Delta x_j \geq 15\,\text{mm}$. However, for a member of length $L = 3600\,\text{mm}$, a resolution of $\Delta x_j = 100\,\text{mm}$ is sufficient. Equation (2) can be written in the form

$$c_j^n v_j^{n+1} - \Delta t_n \Gamma_j^n = \Psi_j^n, \tag{4}$$

where Ψ_j^n does only depend on grid data at time step t_n.

6 Data Assimilation

Equation (4) is solved iteratively in time for v_j^n with a data assimilation step (steps III and IV below) at each iteration. See also the flow chart in Figure 4.

I. Given at time t_n are the values v_j^n on the discretization grid $x_j \in \Sigma_d$ and the collected data as v_j^{n+1} on the thermocouple grid $x_j \in \Sigma_m$;

II. (Assimilation step) Using the collected data v_j^{n+1} at time t_{n+1}, solve (4) for Γ_j^n on the measurement grid $x_j \in \Sigma_m$;

III. Interpolate Γ_j^n to $x_j \in \Sigma_d$. How this interpolant is computed depends on the ansatz for $\Gamma(v, x, t)$, see below;

IV. Solve (4) for v_j^{n+1} on the discretization grid to get temperature distribution at time t_{n+1};

V. Set $n \mapsto n + 1$ and go to step I.

The initial data v_j^1 on the discretization grid, required to start the iteration, is directly interpolated from the collected data on the measurement grid. For the interpolation of Γ_j^n to the discretization grid in step III, we present two different cases:

1. In the simplest case Γ does not depend on the temperature, i.e. $\Gamma = \Gamma(x,t)$. Then a linear interpolation to the discretization grid will do:

$$\Gamma_j^n = \Gamma_k^n + \frac{x_j - x_k}{x_l - x_k}(\Gamma_l^n - \Gamma_k^n) \tag{5}$$

for x_k, x_l on the measurement and x_j on the discretization grid;

2. Newton's law of cooling [10] provides a more realistic model. Here

$$\Gamma = \lambda(x,t)(u_f(x,t) - v(x,t)), \tag{6}$$

where u_f is the furnace temperature and λ the fire protection heat transfer coefficient. On the measurement grid, λ is determined by

$$\lambda_j^n = \frac{\Gamma_j^n}{(u_f)_j^n - v_j^n},$$

and is interpolated to the discretization grid by replacing Γ with λ in (5). Then Γ_j^n on Σ_d is given by

$$\Gamma_j^n = \lambda_j^n((u_f)_j^n - v_j^n).$$

We should note that the data assimilation algorithm I–V is susceptible to noise in the collected data. This does not so much affect the temperature distribution v_j^n as the predicted heat flux Γ_j^n, which may go through enormous fluctuations in time. A simple counter measure is to smooth both the collected data and the heat flux. For example, one could replace the flux after the assimilation step II by

$$\Gamma_j^n \mapsto \frac{1}{\Delta n} \sum_{m=n-\Delta n+1}^{m=n} \Gamma_j^m,$$

that is, by the average heat flux over the last Δn time steps. It is important to note that the data assimilation algorithm modified in this way does not anymore produce an interpolant which matches the collected data at the thermocouple locations. However, this is not a deficiency but a desired property of a robust algorithm.

7 Results

The results in this section are based on a series of fire tests conducted as part of a comparative study of an old and a new, improved furnace, see [7]. The test specimen for two of these tests (Test I in old and Test II in new furnace) was a column of section type HEB180 with a fire protection system consisting of calcium silicate boards. Although a total of 16 thermocouples were used, only 7 thermocouples are non-redundant. Two of these thermocouples measured the temperature of the lower and upper mounts.

For both tests, Figure 5 shows, at different times, the temperature distribution computed by the data assimilation technique in Section 6, where Newton's law of cooling in (6) was used. The vertical lines in Figure 5 mark the location of the thermocouples. Figure 6 shows the dramatic difference between a simple linear interpolation and the data assimilation. Note that the maximal deviation is more than 200C° or 30%. Also note that the maximum of the assimilant can be larger than the highest collected temperature.

The heat flux into the column for Test I is shown in Figure 8 as a surface plot over time and position. Noticeable is that the flux is not monotonically increasing in time. This is due to evaporation of moisture in the fire protection material, which starts at about 20 minutes into the test and lasts 10 minutes. This phase is especially visible in Figure 9, where the total heat flux

$$\Gamma_{total} = \int_0^L \Gamma(x)\, dx$$

is plotted over time.

8 Appendix

To derive Equation (1), we have to assume that the dependence of the material properties $c = c_v \rho$ and k in the lateral direction is negligible, i.e.,

$$c(u(x,y,z,t)) \approx c(v(x,t)) \qquad \text{and} \qquad k(u(x,y,z,t)) \approx k(v(x,t))$$

for all y, z in all x-sections. Then

$$\begin{aligned}
c(v)\partial_t v(x,t) &= \frac{1}{A(\Omega)} \int_\Omega c(v)\partial_t u\, dA \\
&= \frac{1}{A(\Omega)} \int_\Omega \frac{c(v)}{c(u)} \nabla(k(u)\nabla u)\, dA \\
&\approx \frac{1}{A(\Omega)} \int_\Omega \nabla(k(v)\nabla u)\, dA \\
&= \frac{1}{A(\Omega)} \int_\Omega \partial_x(k(v)\partial_x u)\, dA + \frac{1}{A(\Omega)} \int_{\partial\Omega} k(v)\partial_n u\, ds \\
&= \partial_x(k(v)\partial_x v) + \frac{1}{A(\Omega)} \int_{\partial\Omega} \gamma\, ds \\
&= \partial_x(k(v)\partial_x v) + \Gamma.
\end{aligned}$$

References

[1] G. Anger, Inverse Problems in Differential Equations, Plenum Press, 1990

[2] P. Deuflhard, E. Hairer (ed.), Numerical Treatment of Inverse Problems in Differential Equations, Proceedings, 1982 J 2.0 — 82 Hei 1

[3] DIN 4102, Part 2, Behavior of Building Materials and Components in Fire; Building Components; Definitions, Requirements, and Tests, Edition 09.77, Beuth Verlag GmbH, Berlin, Köln, 1991.

[4] Ghil, Michael, and Paola Malanotte-Rizzoli Data Assimilation in Meteorology and Oceanography, Advances in Geophysics, 33, pp. 141–266, 1991.

[5] Grewal, M.S. and A.P. Andrews Kalman Filtering Theory and Practice, Prentice-Hall, Englewood Cliffs, New Jersey, 1993.

[6] J. L. Lions, Optimal Control of Systems Governed by Partial Differential Equations, Springer, 1971

[7] Z. F. Pan, R. Schriever, H. M. Block and M. Korzeń, Comparison of the Temperature Distribution in Isolated Steel Columns Tested in Two Furnaces, Fire Technology, Vol. 33, No. 4, 1997

[8] prENV YYY5-4:1998, Test Method for Determining the Contribution to the Fire Resistance of Structural Members Part 4: Applied Protection to Steel Members, European Committee for Standardization, Brussels, 1998.

[9] Press, Flannery, Teukolsky and Vetterling, Numerical Recipes, Cambridge University Press, 1986

[10] S. Whitaker, Elementary Heat Transfer Analysis, Pergamon, New York, 1976

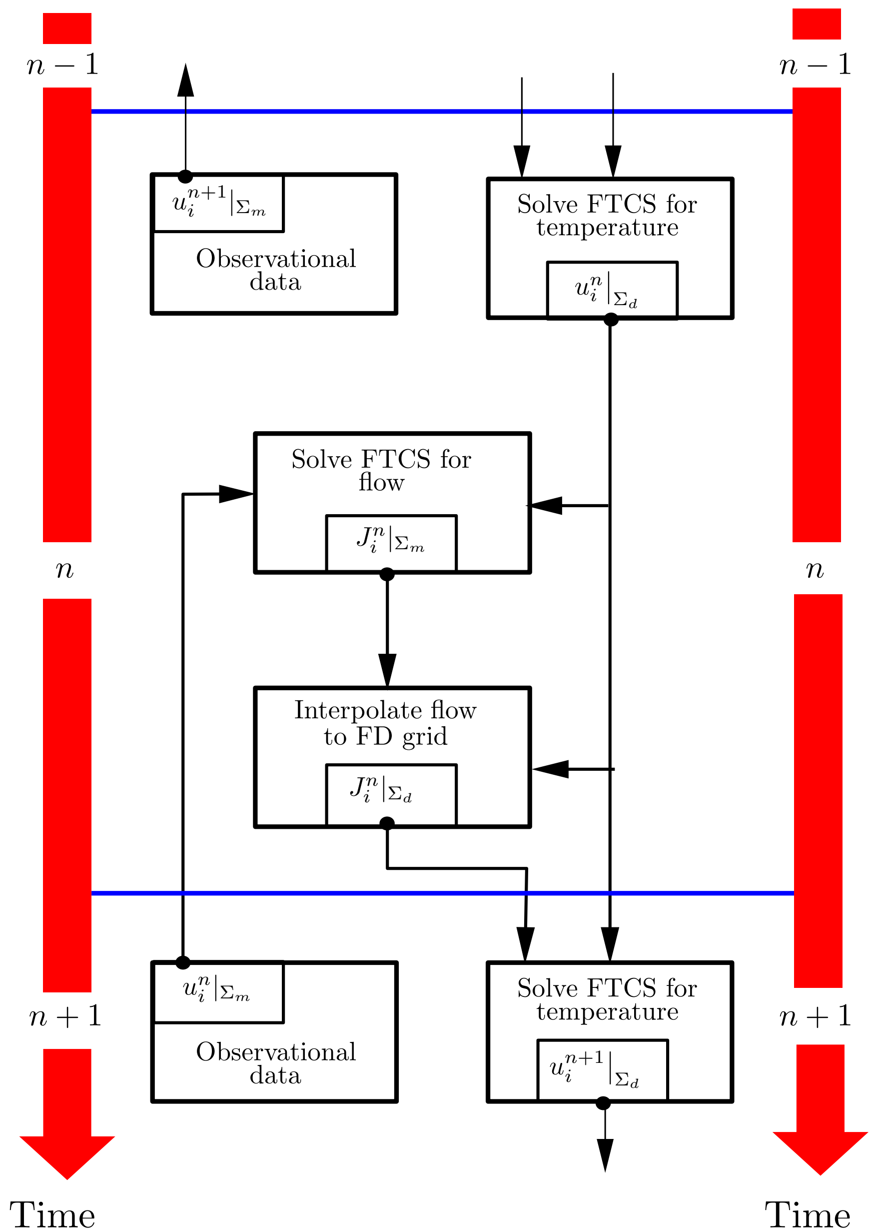

Figure 4: Overview of time-sequential assimilation process

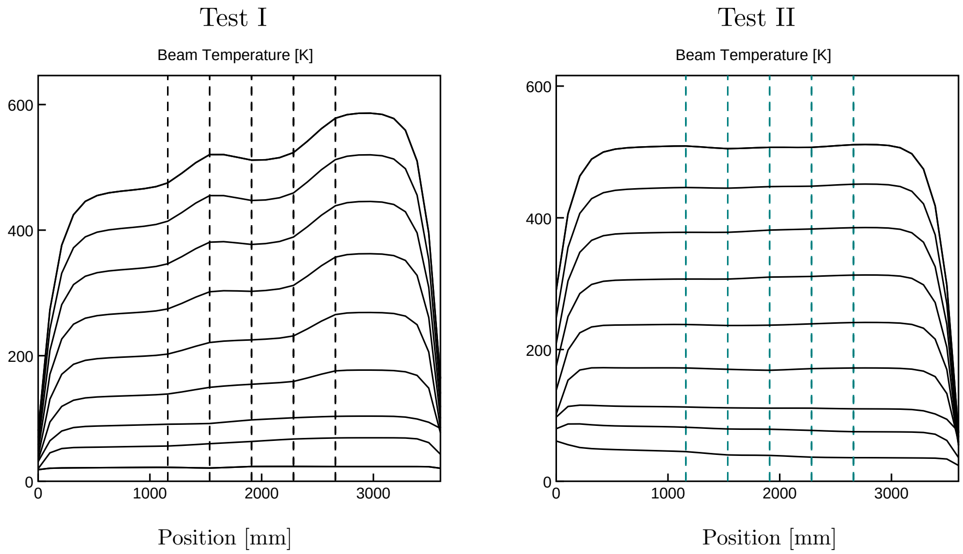

Figure 5: Temperature Distribution by Assimilation on Test I (old furnace) and Test II (new furnace) in 10 minutes intervals

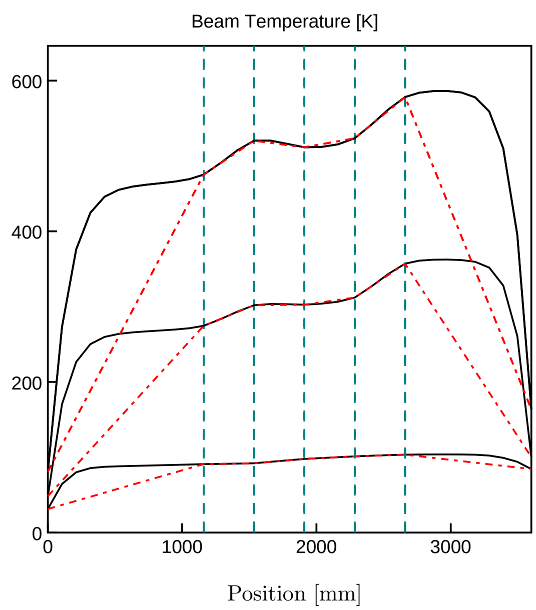

Figure 6: Linear Interpolant and Assimilant for Test I in 30 minutes intervals

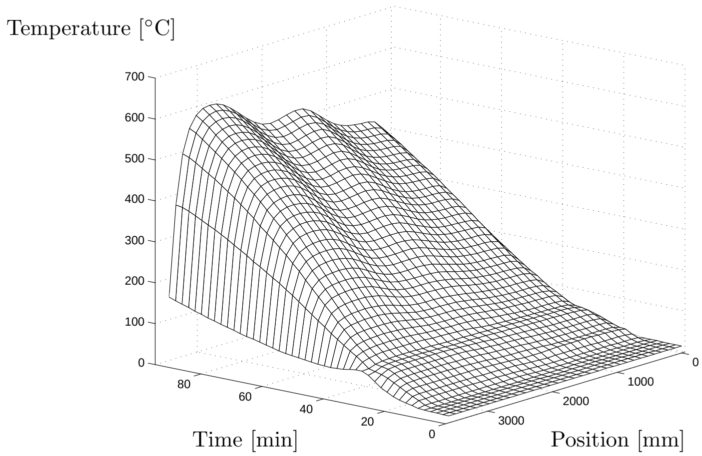

Figure 7: Temperature distribution for Test I over time and position

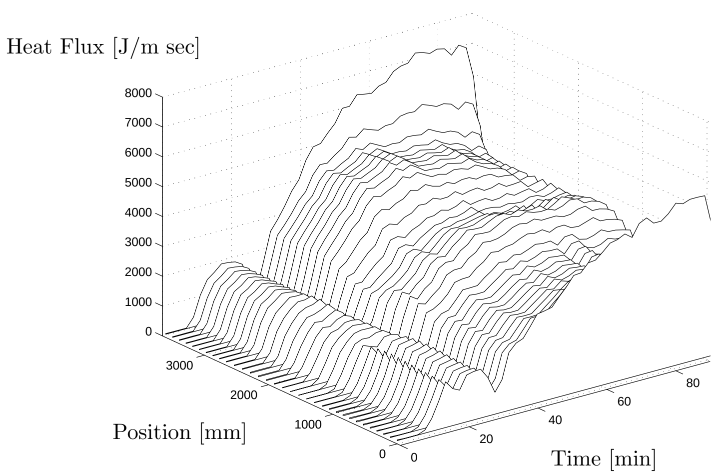

Figure 8: Heat flux line density for Test I over time and position

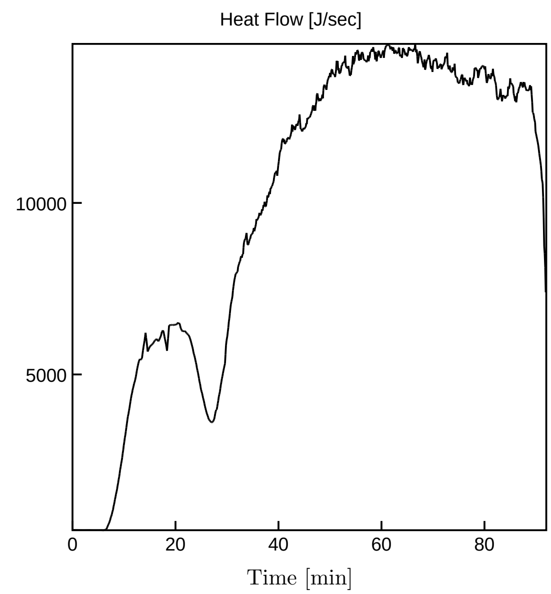

Figure 9: Total heat flux Γ_{total} over time for Test I